Journal Name

RSCPublishing

ARTICLE

Novel Thermosensitive Telechelic PEGs With Antioxidant Activity: Synthesis, Molecular Properties and Conformational Behaviour

Cite this: DOI: 10.1039/xoxxoooooox

Received ooth January 2012,
Accepted ooth January 2012

DOI: 10.1039/xoxxoooooox

www.rsc.org/

Olga Sergeeva,[a] Petr S. Vlasov,[a] Nina S. Domnina,[a] Anna Bogomolova,[b] Peter Konarev,[c] Dmitri I. Svergun,[c] Zuzana Walterova,[b] Jiri Horsky,[b] Petr Stepanek[b] and Sergey K. Filippov*[b]

We report on the synthesis and solution properties of novel tailor-made polymer conjugates, which are highly compelling for biomedical applications due to their antioxidant activity and the potential to fine-tune their thermosensitive properties. These conjugates consist of polyethylene glycol (PEG polymers containing antioxidant moieties, namely 3-(3,5-di-*tert*-butyl-4-hydroxyphenyl)propionate or 2-benzamido-3-(3,5-di-tert-butyl-4-hydroxyphenyl)acrylate, as end groups that differ in activity and hydrophobicity. It was shown that all of the synthesised conjugates have low critical solution temperatures (LCSTs) characteristic of type II polymers on a phase diagram. By simply varying the PEG molecular weight, the solution properties, including the LCST value, could be easily tuned across a broad temperature range of 20-90 ºC, providing an ideal method for the creation of thermosensitive polymers. It was also established that the LCST value and the polymer conjugate conformation depend on the antioxidant structure. From dynamic light scattering and small-angle X-ray scattering data, we were able to construct a complete sequence diagram of the conformational phase behaviour for the polymers with increasing temperature. It was observed that the conjugate conformation changes are the result of water shifting from a thermodynamically favourable solvent to an unfavourable one. This process then leads to compaction of the conjugate, followed by its aggregation.

Introduction

For several decades, there has been a continuous quest for polymer conjugates with enhanced biological properties,[1-5] antioxidant activity being one such property. The application of antioxidants is of great importance for human health.[6-8] Nevertheless, their applicability is limited by their solubility in organic and aqueous media because commonly known antioxidants are either lipophilic or hydrophilic. It has been suggested that amphiphilicity may be beneficial for the potential application of these molecules.[9] To achieve this property, the conjugation of a hydrophobic antioxidant moiety with a hydrophilic or amphiphilic polymer appears logical. This approach has been applied successfully to a variety of tasks, yielding a number of new biocompatible and biodegradable compounds.[10-23]

Taking into account potential biomedical applications, the solution properties of these amphiphilic polymers must be thoroughly investigated. The combination of a low-solubility hydrophobic drug with a hydrophilic polymer can drastically alter the final conjugate's phase diagram in water. It is known that all non-ionic water soluble polymers have a low critical solution temperature (LCST), the point on a phase diagram at which the solubility of the polymers increases with decreasing temperature. The polymer concentration corresponding to the LCST value on a phase diagram can sometimes be varied by

changing the length of the polymer chain. Polymers whose LCST value decreases with increasing molecular weight are known as type I, whereas polymers of type II have LCST positions that are insensitive to molecular weight.[24-32] For some water soluble polymers, such as PEG,[24] poly(2-methyl-2-oxazoline) (pMeOx), and poly(*N*-(2-hydroxypropyl) methacrylamide (pHPMA), the LCST value is above 100 ºC, making them soluble at temperatures below water's boiling point. Polymers whose phase behaviour changes in solution as a response to variations in the environmental temperature are called thermosensitive polymers.[33] Polymers that demonstrate these changes at body temperature (37-40 °C) are particularly important in biomedical, cosmetic and pharmaceutical applications. In particular, temperature-responsive polymers can find application as in situ gel-forming drug delivery systems,[34,35] and for formulating poorly soluble drugs.[36] Poly(N-isopropylacrylamide) (PNIPAAm), poly(vinyl methyl ether) (PVME), and some polyalkyloxazolines[37] are well-known thermosensitive polymers that are fully soluble in water at lower temperatures but undergo phase separation above 32 ºC, resulting in the formation of a turbid suspension. Modifying highly soluble polymers such as pMeOx, pHPMA, PEG, starches, or dextran with hydrophobic or thermosensitive moieties lowers their LCST values.[28,29,32,34,36,38-52] Polymers architecture and grafting density might have also influence on thermosensitive properties.[48,51,53-55]

In the majority of studies on polymers with LCST behaviour, the hydrophobic or thermosensitive modifier possesses no biological activity. Moreover, controlling the LCST value by varying the substituent's hydrophobicity is not straightforward. A polymer that combines thermosensitivity with the propensity to scavenge free oxygen radical species (i.e., antioxidant activity) is a unique combination with great potential for biomedical applications. In this paper we report on the synthesis of conjugates that are both thermosensitive and able to work as antioxidant substances. Through a combination of methods including dynamic light scattering (DLS), and small angle X-ray scattering (SAXS), the solution properties of the conjugates were thoroughly investigated. DLS provides information on the size (i.e., hydrodynamic radius) of nanoparticles in solution.[56] SAXS was used to obtain essential information on the structure of the thermoresponsive antioxidant polymer conjugates; by curve-fitting the SAXS data, detailed information on the polymer solution properties (e.g., size (gyration radius), shape, and conformation structure (related to excluded volume effects)) was collected. SAXS served as a powerful tool for analysing nanoparticle structures and suspensions of both concentrated and diluted polymer solutions.[46,57-60] It was shown that through simple variation of the PEG fragment length, the LCST value could be adjusted to any temperature required for biomedical applications.

Experimental

Materials

Reagent-grade solvents and reagents were purchased from a local reseller (Vekton) and purified using conventional procedures. Benzene, chloroform, diethyl ether, and petroleum ether were distilled over phosphorous pentoxide; thionyl chloride was purified by distillation over linseed oil in an argon atmosphere. 2-propanol, 4-Dimethylaminopyridine (DMAP) and triethylamine (Et_3N) were used as-received after testing for impurities was used as-received after testing for impurities.

Polyethylene glycols (PEGs, M_n = 2k, 3k, 4k, 6k and 20k) were provided by Prof. N. M. Geller (IMC Russian Academy of Science), purified by precipitation from benzene into diethyl ether and dried under high vacuum with phosphorous pentoxide.

3-(3,5-di-*tert*-butyl-4-hydroxyphenyl)propanoyl chloride (compound A) was prepared from 3-(3,5-di-*tert*-butyl-4-hydroxyphenyl)propanoic acid (fenozan acid, Vekton); the acid also served as model compound MA and was recrystallised from dry chloroform, then dried under high vacuum before use. Compound MA (2.25 g, 8.1 mmol) and thionyl chloride (0.9 mL, 12.4 mmol) were refluxed in chloroform (20 mL) for 4 h. After evaporation of the solvent and excess thionyl chloride under vacuum, the product was isolated as a slightly yellowish solid (98%, m.p. 66-68 °C).

4-(3,5-di-*tert*-butyl-4-hydroxybenzylidene)-2-phenyloxazol-5(4H)-one (compound B), was prepared according to Ref. 61 (m.p. 214-215 °C).

UV-Vis spectra were recorded in water-ethanol solution (1:1 v/v) at ambient temperature using a Shimadzu UV-1700 spectrometer (Figure 1). The molar extinction values at D_{max} obtained for the model compounds MA and MB, ε_A=1700±30 (276 nm) and ε_B=22800±400 (320 nm), were used to calculate the quantities of introduced fragments in the PEG-A and PEG-B.

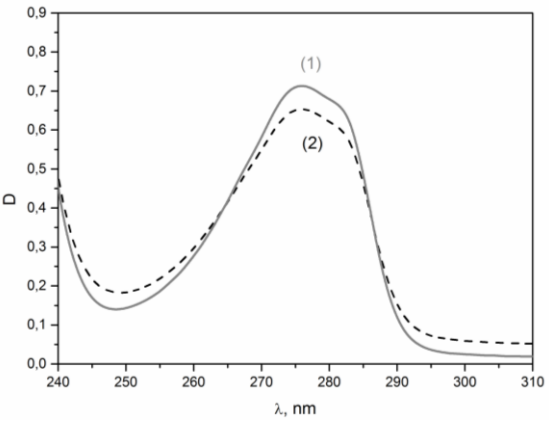

Fig. 1 UV spectra of (1) model compound MA C=4.2×10^{-4} mol/L (0.12 g/L) and (2) the telechelic PEG-A polymer (6k) χ=7.6 mass %, C=5.1×10^{-3} mol/L (1.41 g/L).

Oxazolone B (0.302 g, 0.80 mmol) in chloroform (1.5 mL) was added to PEG-6k (0.3 g, 0.10 mmol), DMAP (0.0586 g, 0.48 mmol) and triethylamine (0.04 mL, 0.32 mmol) in 1.5 mL of chloroform under argon. After stirring at 60 °C for 48 h, the product was isolated by precipitation in a mixture of 2-propanol, petroleum ether, and diethyl ether (2:1:1, v). In order to remove any trace of reagents and minimize the loss of the polymer, the product was fist dried, then washed with an acetone and petroleum ether (1:1, v) and then precipitated from chloroform into the acetone and petroleum ether mixture. After removing volatiles under high vacuum, the product became a slightly yellow-coloured powder (0.18 g, 55%).

Dynamic Light Scattering (DLS)

To obtain detailed knowledge of the particle distribution in solution, measurements were carried out on an ALV instrument equipped with a 22 mW He-Ne laser at a 90° angle. The

resultant correlation functions were analysed by REPES,[62] an analytical software that provides the distribution function of hydrodynamic radii ($G(R_h)$). To account for the logarithmic scale on the R_h axis, all DLS distribution diagrams are shown in the equal area representation $R_hG(R_h)$.[63] For all experiments, approximately 2 mL of the sample solution was filtered using a 0.22 μm PVDF filter and transferred to a sealed, dust-free light scattering cell. The temperature was controlled within 0.05 °C. The apparent hydrodynamic radius of the nanoparticles (R_h) was calculated using the Stokes-Einstein equation.

Cloud point temperatures (CPT) for each concentration were determined from the temperature dependence of the particle hydrodynamic radius, R_h, and the scattering intensity, I_s, measured at the scattering angle θ=173° on a Zetasizer Nano-ZS, Model ZEN3600 (Malvern Instruments, UK). For data evaluation, the DTS (Nano) program was used.

Small Angle X-ray Scattering (SAXS)

Synchrotron SAXS experiments were performed at the EMBL beam line P12 (Petra III, Hamburg, Germany) using a pixel detector (2M PILATUS). The X-ray scattering images were recorded for a 3.1 m sample-detector distance, using a monochromatic incident X-ray beam (λ = 0.125 nm) covering a momentum transfer range of 0.05 $nm^{-1} < q < 4.5$ nm^{-1} ($q = 4\pi\sin\theta/\lambda$, where 2θ is the scattering angle). The majority of the samples showed no measurable radiation damage upon comparing twenty successive time frames with 50 ms exposures. In all instances reported in this paper, the two-dimensional scattering patterns were isotropic. These patterns were azimuthally averaged to yield the dependence of the scattered intensity ($I_s(q)$) on the momentum transfer (q). Prior to the fitting analysis, the solvent scattering was subtracted.

All SAXS data manipulation was performed using the PRIMUS software.[64] The forward scattering ($I_s(q=0)$) and the radius of gyration (R_g) were evaluated using the Guinier approximation. For further modelling, the data were adjusted to an absolute scale by subtracting the results of an empty cell measurement from those of a pure water measurement and scaling by the ratio of the theoretical forward scattering of water to the experimental forward scattering intensity of water. Experiments were conducted in a temperature range of 14-45 °C using an experimental setup described previously.[65] For clarity, some of the SAXS curves were binned to reduce noise at the high-q range.

MALDI–TOF Mass Spectrometry

The samples were prepared using the dried droplet method,[66] where the sample solution (10 mg/mL) was added to DHB (2,5-Dihydroxybenzoic acid, 20 mg/mL) as a matrix with sodium chloride (NaCl, 10 mg/mL) in H_2O as a cationisation agent and mixed in a 4:20:1 volume ratio. A 1 μL aliquot of the mixture was deposited on the ground steel target plate and dried under an ambient atmosphere.

MALDI-TOF mass spectra were acquired with the new UltrafleXtreme TOF/TOF mass spectrometer (Bruker Daltonics, Bremen, Germany) in the positive ion reflectron mode for the PEG-3, 4 and 6k, and in the linear mode for the PEG-20k. The spectra were the sum of 30,000 pulses with a DPSS Nd:YAG laser (355 nm, 1000 Hz). For these measurements, both delayed extraction and external calibration were used.

Results and discussion

Telechelic polyethylene glycols were synthesised from PEGs using chemical modification of their hydroxyl end groups. For the synthesis of PEG-A_2, the chloro anhydride A was produced from the precursor acid MA and used the same day (Scheme 1). Both the reaction conditions and the ratio of A to the end groups were varied to achieve the full conversion, shown in Table 1. It was found that heating at 40 °C for 6 h was insufficient to transform all of the end groups, thus requiring an additional overnight stirring. After that point, there was no further increase in the A-fragment content, even after additional heating. As the OH end group concentration was lower in the higher molecular weight PEG, the ratio of compound A to PEG was necessarily increased.

The reaction of PEG with compound B proceeded via oxazolone ring opening, requiring a base catalyst. The reaction conditions and bases used were optimised on PEG-6k, shown in Table 2 (Scheme 2). A higher number of B fragments was observed when two bases were combined, i.e., DMAP and Et_3N. Although a higher temperature (60 °C) and longer reaction time (48 h) than those used for A were applied, full end-group conversion was achieved only for the PEG-2k. For the other PEGs, the degree of substitution (DS) was c.a. 0.7. Thus, the product comprises a mixture of the telechelic PEG-B_2 and a semi-telechelic PEG-B_1. We decided to avoid separating the two because this process would lead to dramatic product loss. However, an investigation of the collective physical properties was performed, as the mixture may still be suitable for an application.

The structure of PEG-A_2 and PEG-B was confirmed by NMR and MALDI-TOF spectra (Figures 2, 3). The initial PEGs and the telechelic PEG-A and PEG-B were observed in the MALDI-TOF MS as sodium cation adducts. Table 4 shows good agreement between the theoretical and observed molecular mass values. The molar ratio was estimated from the mass spectra for PEG-B_2/PEG-B_1, and from that, the DS. These results are presented in Table 3.

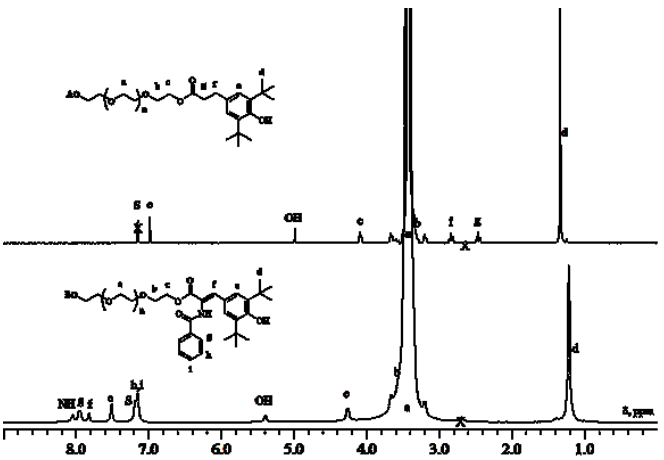

Fig. 2 ^{1}H NMR spectra of the products PEG-A (6k) and PEG-B (6k) in C_6D_6.

The proton NMR spectra of PEG-A_2 and PEG-B (Figure 2) clearly show the presence of the corresponding A and B fragments. According to our previous experience, the best signal resolution in ^{1}H NMR for PEG-derivatives is observed when using deuterated benzene. The intensity ratio of the signal at δ=3.5 ppm (PEG) and that of the singlet at 1.2-1.3 ppm (*tert*-butyl groups) gave the average degree of substitution,

corresponding to the observed MALDI-TOF values. The chemical bond between the introduced fragment and polymer was confirmed by the PEG methylene group to carboxyl group triplet at δ=4.09 ppm for PEG-A, and at 4.26 ppm for PEG-B. The assignments of the carbon spectra peaks are given in the experimental section.

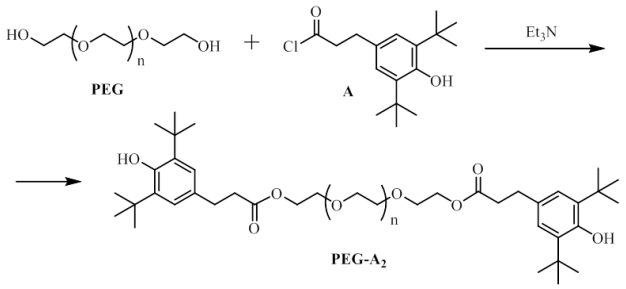

Scheme 1 The synthesis and structure of the PEG-A conjugates.

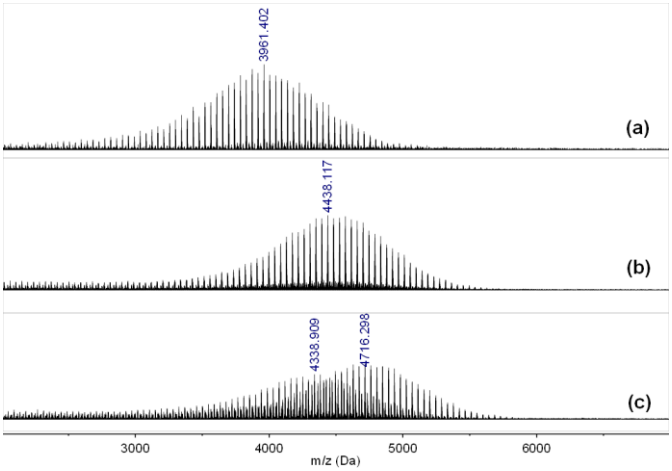

Fig. 3 MALDI-TOF spectra of (a) PEG-4k, (b) PEG-A(4k), and (c) PEG-B(4k).

Table 1 Reaction conditions for the PEG-A synthesis

N	PEG [a]	[**A**] / [OH] [b]	T, h [c]	χ, mass % [d]	Yield, % [e]
1	2k	3	4	6.1	30
2		3	6 *	**19.8**	29
3	3k	3	4	8.4	61
4		3	6	13.5	58
5		3	6 *	**15.7**	59
6	4k	3	4	6.2	68
7		3	6 *	10.8	66
8		6	4	8.7	65
9		6	6 *	**13.9**	66
10	6k	6	4	4.2	76
11		6	6 *	**7.6**	74
12	20k	6	6 *	1.2	77
13		9	6 *	2.2	78
14		12	6 *	**3.2**	77

[a] approximate initial M_n of the PEG, PEG concentration in the mixture was c.a. 10 mass %; [b] molar ratio of reagent A to OH end-groups; [c] heating time at 40°C, asterisk shows overnight stirring at r.t.; [d] mass fraction of the introduced fragments, numbers in bold shows the investigated samples; [e] yields were calculated, taking into account the change in MM.

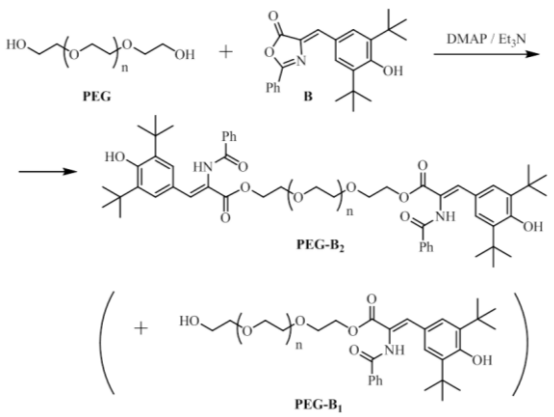

Scheme 2 The synthesis and structure of the PEG-B conjugates

Table 2 Reaction conditions of the PEG-B synthesis

N	PEG[a]	B[b]	DMAP[b]	Et_3N[b]	χ, mass %[c]	Yield, %
1	2k	5	3	2	26.5	42
2	4k	7	4	3	13.4	52
3	6k	8	2	0	5.2	56
4		8	10	0	8.2	56
5		8	0	10	5.1	54
6		8	6	4	8.5	55
7	20k	15	9	6	2.2	68

[a] approximate initial M_n of the PEG, PEG concentration in the mixture was c.a. 6 mass %; [b] per 1 OH end-group; [c] mass fraction of the B fragments.

Table 3 Properties of the resultant products

	M_n [a)]	χ, mass % [b)]	DS_{UV} [c)]	M_n [d)]	DS_{MALDI} [e)]
PEG	2k			2097 (1.01)	
	3k			3428 (1.04)	
	4k			3929 (1.01)	
	6k			6678 (1.005)	
PEG-A	3k	15.7	c.a. 1	3842 (1.04)	c.a. 1
	4k	13.9	c.a. 1	4221 (1.03)	c.a. 1
	6k	7.6	c.a. 1	7053 (1.006)	c.a. 1
PEG-B	2k	26.5	0.953	2826 (1.01)	0.958
	4k	13.4	0.818	4278 (1.03)	-
	6k	8.5	0.737	7097 (1.005)	0.627

[a)] approximate molecular mass M_n according to manufacturer; [b)] mass fraction of the introduced fragments; [c)] degree of OH end group substitution in the PEG from UV-Vis; [d)] average molecular mass and molar mass dispersity ($Đ = M_w/M_n$) calculated from the MALDI TOF; [e)] degree of substitution calculated from the MALDI TOF.

Table 4 MALDI results for the oligomer components in the PEG (6k) derivatives, ionised with sodium ions

DP[a)]	**$[PEG\text{-}A_2+Na]^+$**		**$[PEG\text{-}B_2+Na]^+$**		**$[PEG\text{-}B_1+Na]^+$**	
	Calc.	Found	Calc.	Found	Calc.	Found
50	2762.666	2762.588	2996.709	2996.247	2619.510	2619.498
60	3202.928	3202.879	3436.971	3437.066	3059.772	3059.802
70	3643.191	3643.219	3877.234	3877.439	3500.034	3500.133
80	4083.453	4083.614	4317.496	4317.859	3940.297	3940.510
90	4523.715	4523.012	4757.758	4757.347	4380.559	4380.945
100	4963.977	4963.533	5198.020	5198.839	4820.821	4821.438
110	5404.239	5404.171	5638.282	5638.620	5261.083	5261.970

[a)] degree of polymerisation.

ARTICLE

Having established the chemical structure of the conjugates, the solution properties of the PEG, PEG-A, and PEG-B conjugates in water were determined using DLS. The intensity-weighted distribution function for the PEG-A(4k) conjugate unambiguously shows that the conjugate has thermosensitive properties. With increasing temperature, the dominant peak with a R_h of 2-3 nm shifts to a higher R_h value (Figure 4). This peak can be attributed to single polymer chains. A small fraction of the molecules form aggregates at low temperatures, and at T=42 ºC, a new peak with considerably higher R_h values begins to dominate the intensity-weighted distribution function, implying the existence of large aggregates in the solution. A similar behaviour was observed for the PEG-A (3k) sample (Supporting Information, Figure 1S).

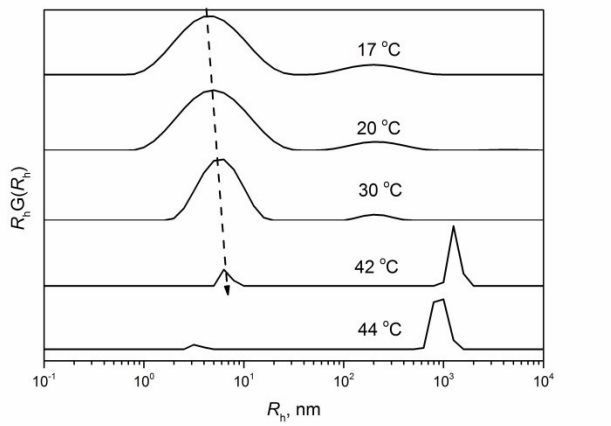

Fig. 4 Intensity-weighted distribution function obtained from the DLS data for PEG-A (4k) conjugate at different temperatures; C=1.0 wt%.

Large aggregates begin to appear at the cloud point temperature. The sub-micron size of the new peak results from precipitation of the polymer conjugate molecules from the solution.

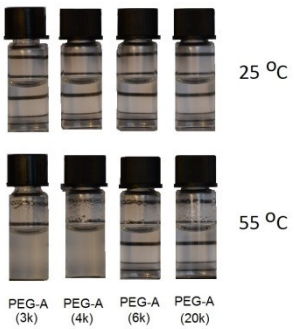

Fig. 5 The pictures of solutions of the conjugates PEG-A at temperatures T=25 ºC and T=55 ºC; C=1.0 wt%.

Visual inspection confirms thermosensitivity of the conjugates (Figure 5). Heating at T=55 °C makes the solutions of the PEG-A(3k) and PEG-A(4k) conjugates turbid. Further heating above 75°C makes PEG-A(6k) conjugate also opaque in contrast with PEG-A(20k) conjugate that stays transparent even above 85 °C. To find the precise CPT position for each concentration, the dependence of the scattered intensity and R_h at each particular concentration were monitored as a function of temperature (Figure 6 A, B; Supporting Information Figure 2S, 3S).

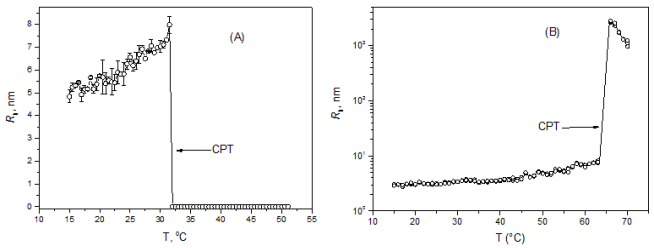

Fig. 6 The R_h value temperature dependence obtained from the intensity-weighted distribution functions for (A) PEG-A (3K) and (B) PEG-A (6K); C=1.0 wt%.

Both the intensity and the R_h exhibit divergence at a specific point, corresponding to the CPT. Two features could be noted: the R_h value increases as it approaches the CPT, and the CPT value depends on the PEG's molecular weight. The growth of the hydrodynamic radius can be explained by in two ways. One possible explanation is that continuous aggregation takes place as the temperature approaches the CPT. A second explanation comes from the nature of the apparent translational diffusion coefficient (inversely proportional to the hydrodynamic radius), which is influenced by a second virial coefficient. It has been shown[67] that in dilute solutions, the concentration-dependant diffusion coefficient (k_D) is related to the second viral coefficient (A_2) and molecular weight (M_w) by the following equation:

$$k_D = 2A_2M_w - k_f - \bar{\upsilon} \quad (1)$$

where k_f and υ are the friction coefficient and partial specific volume, respectively. In contrast to A_2, k_f is always positive, therefore the sign of k_D is generally determined by all three parameters: M_w, A_2, and k_f (the partial specific volume can be neglected). When the thermodynamic quality of the solvent worsens, the apparent value of R_h increases at finite concentrations as a result of the decreasing value of A_2. We do not present this as an explanation of the R_h increase but to show that the temperature effect on R_h at finite concentrations is more complex than at an infinite dilution. The CPT dependence on the PEG's molecular weight can easily be explained by a change in the hydrophilic/hydrophobic ratio.

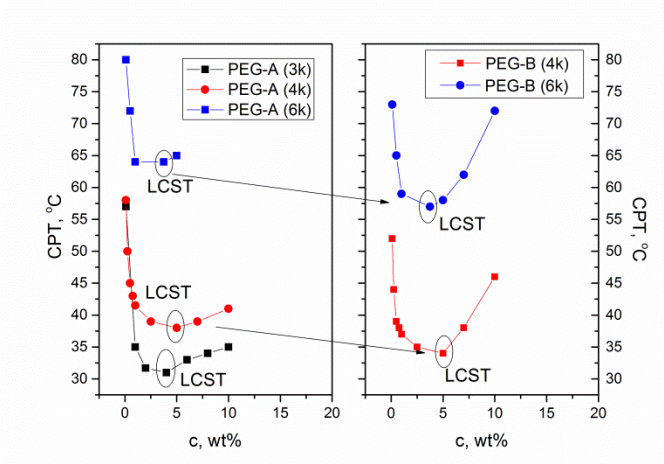

Fig. 7 A phase diagram of the PEG-A and PEG-B conjugates with different PEG molecular weights.

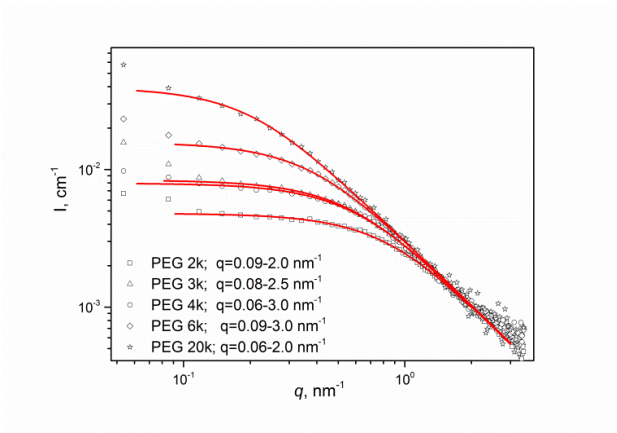

Fig. 8 SAXS curves for PEG solutions with different molecular weights taken at T=25.3 °C; C=2.0 wt%. The solid lines are fits in the appropriate fitting range.

A complete phase diagram of the polymer solution can be obtained from the plot of the CPT value as a function of concentration. It can be seen from Figure 7 that the phase diagram for the PEG-A conjugate possesses a minimum that could be described as the LCST. The LCST value is dependent on molecular weight; for PEG-A (6k), it is nearly twice that of PEG-A (3k) (Figure 6A). It can be observed that the position of LCST does not depend on the molecular weight of PEG with the limits of experimental error, allowing us to classify the phase diagram of the PEG-A conjugates as type II. However, we admit that LCST temperature dependence may appear if higher PEG molecular weights are used. For a robust analysis of this phenomenon, a molecular weight range across at least two orders of magnitudes should be used.[24] Unfortunately, at higher PEG M_w, the CPT value will exceed water's boiling point. Finally, we have seen that the LCST value depends on the antioxidant structure. The PEG-B conjugates have lower LCST values for the same PEG molecular weight (Figure 7). The LCST drop to lower values is caused, obviously, by higher substituent's hydrophobicity.

Next, the detailed structures of the modified and unmodified polymers were investigated by SAXS. The unmodified PEGs were measured at T=25.2 ºC and concentrations of 0.5, 1.0, and 2.0 wt% (Figure 8, Table 5). Measurements at concentrations below 0.5 wt% were problematic due to the low scattering intensity of the polymer solution. Using the Guinier analysis, the apparent radius of gyration (R_g) for the conjugates was estimated (Table 5). The effect of the polymer concentration on the R_g is shown in Figure 9. The slopes of the lines for R_g vs. c are related to the second virial coefficient, and negative and positive slopes indicate repulsive and attractive polymer interactions, respectively. The PEG macromolecules exhibited only repulsive interactions (the positive second virial coefficient) due to steric repulsion. By extrapolating the R_g to infinite dilution, one can calculate the true gyration radius that increases with increasing PEG molecular weight. Furthermore, to estimate the solution parameters, a generalised Gaussian model with excluded volume effects[68] was used to fit the polymer SAXS data (Figure 7). This fitting model provided the gyration radius (R_g), the excluded volume parameter (υ), and the scattered intensity extrapolated to zero (q) (Tables 5-7). The excluded volume parameter υ varies in the range of 0.33–1.0, with a υ value of 0.5 standing for theta (solvent).
standing for theta (solvent).

Table 5 The fitting parameters from SAXS. T=25.3 ºC for non-modified PEGs.

polymer	C, wt.%	R_g, Guinier, nm	R_g, nm	ν	χ^2
PEG 2k	0,5	4.7 ± 1.7	3,0	0,77	0.83
PEG 2k	1	1.7 ± 0.5	2.0	0,68	0.98
PEG 2k	2	1.4 ± 0.4	1,6	0,59	0.98
PEG 3k	0,5	-	3,2	0,69	0.83
PEG 3k	1	2.3 ± 0.5	2,5	0,62	0.94
PEG 3k	2	1.9 ± 0.5	2,4	0,61	1.04
PEG 4k	0,5	3.2 ± 0.9	3,7	0,71	0.89
PEG 4k	1	1.5 ± 0.8	2,8	0,71	0.80
PEG 4k	2	1.9 ± 0.4	2,3	0,61	1.01
PEG 6k	0,5	5.1 ± 2.1	5,2	0,67	0.91
PEG 6k	1	2.7 ± 0.9	3,3	0,57	0.87
PEG 6k	2	3.2 ± 0.7	3,6	0,62	1.03
PEG 20k	0,5	5.0 ± 1.5	9,2	0,71	0.73
PEG 20k	1	5.4 ± 1.5	6,8	0,69	0.86
PEG 20k	2	5.5 ± 1.6	6,6	0,63	1.03

The acquired fitting parameters corroborate the conclusions drawn from the apparent R_g concentration dependence. The excluded volume parameter for the PEGs indicates that at T=25 ºC, all polymers are swollen in water, revealing that it is a thermodynamically favourable solvent (Table 5).

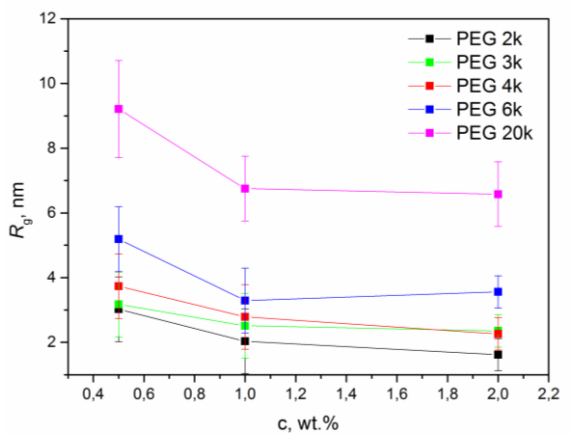

Fig. 9 R_g concentration dependence for the unmodified PEGs.

The conformation properties of the modified polymers were studied across the temperature range of 15-45 ºC (Figure 10, Tables 6 and 7). All polymers had a 1.0 wt% concentration due to the low scattering of dilute polymer solutions. Using the generalised Gaussian coil model, all SAXS data were successfully fitted (Figure 10). For some polymer systems, (Figure 10) the presence of aggregates was visible at low q ranges. The existence of large aggregates was also observed by DLS. In these instances, the fitting was performed only on the part of the SAXS curve that was free of aggregate scattering. The fitted functions were later simulated for the complete q range (Figure 10).

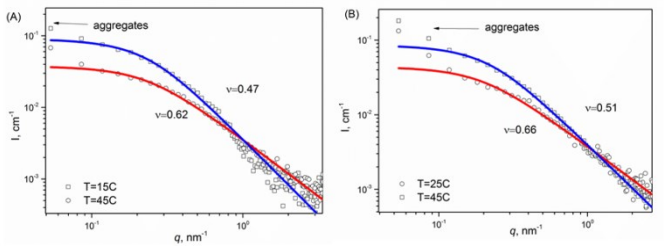

Fig. 10 SAXS curves for modified PEG solutions taken at different temperatures for (A) PEG-A (4k) and (B) PEG-B (6k); C=1.0 wt%. The solid lines are fits.

The SAXS experiments unambiguously indicate conformational changes of the polymers as they approach the CPT (Figure 9). Figure 11 (A, B) shows that the apparent particle sizes increase as they approach the CPT. The same phenomenon was observed for the hydrodynamic radius measured using DLS (Figure 6).

Table 6 The fitting parameters from SAXS for PEG-A conjugate; C=1.0 wt%.

polymer	T, ºC	R_g, nm	ν	χ2
PEG-A (3k)	15,4	4,85	0,47	1.12
PEG-A (3k)	20,3	5,05	0,43	1.06
PEG-A (3k)	25,3	5,72	0,42	0.98
PEG-A (3k)	45,5	precipitation	--	
PEG-A (4k)	15,1	5,71	0,62	0.92
PEG-A (4k)	20,4	5,71	0,61	1.02
PEG-A (4k)	25,3	-	0,51	0.89
PEG-A (4k)	35,3	6,26	0,44	0.99
PEG-A (4k)	45,2	6,55	0,47	0.97
PEG-A (6k)	25,2	6,65	0,66	0.95
PEG-A (6k)	35,3	5,74	0,65	0.76
PEG-A (6k)	45,3	precipitation	-	
PEG-A (20k)	25,2	11,7	0,66	0.79
PEG-A (20k)	35,3	13,1	0,68	0.77
PEG-A (20k)	45,3	14,4	0,61	0.89

Table 7 The fitting parameters from SAXS for PEG-B conjugate; C=1.0 wt%.

polymer	T, ºC	R_g, nm	ν	χ2
PEG-B (2k)	15,4	3,76	0,37	0.77
PEG-B (2k)	20,3	3,57	0,30	1.00
PEG-B (2k)	25,3	3,90	0,30	1.41
PEG-B (2k)	35,2	3,90	0,36	0.85
PEG-B (2k)	45,2	2,82	0,33	0.96
PEG-B (4k)	15,4	5,00	0,47	0.90
PEG-B (4k)	25,3	5,48	0,43	0.89
PEG-B (4k)	35,2	5,69	0,41	1.74
PEG-B (4k)	45,2	6,41	0,39	1.47
PEG-B (6k)	25,3	6,64	0,67	0.97
PEG-B (6k)	35,2	6,55	0,59	0.94
PEG-B (6k)	45,2	6,78	0,52	1.03
PEG-B (20k)	25,3	22,6	0,69	0.92
PEG-B (20k)	35,2	-	0,71	0.98
PEG-B (20k)	45,2	18,8	0,67	1.08

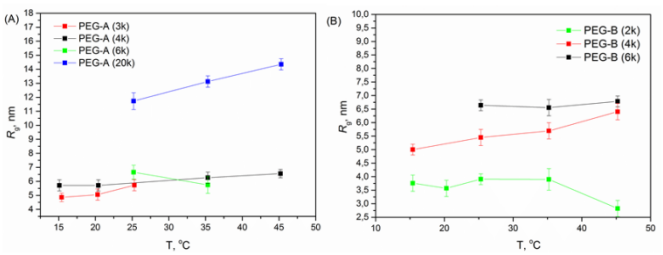

Fig. 11 R_g temperature dependence for conjugate solutions of (A) PEG-A and (B) PEG-B; C=1.0 wt%.

As the apparent R_g value depends on the second virial coefficient, we are inclined to attribute the growth of the R_g to the worsening thermodynamic quality of the solvent rather than the aggregation of the conjugates. This conclusion is further supported by the dependence of υ on temperature (Figure 12). The PEG conjugate conformation can be easily controlled by a simple variation of the PEG's chain length. As can be seen from decline of the υ value, for the PEG-B (6k) and PEG-A (4k) polymers, the transition from a swollen Gaussian coil to a contracted coil was observed, whereas the PEG-B (20k) and PEG-A (20k) conjugates only existed as swollen Gaussian coils in solution.

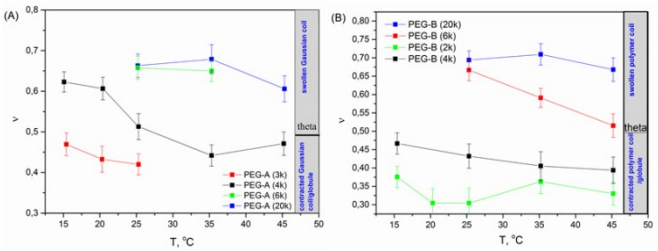

Fig. 12 Temperature dependence of the excluded volume parameter for solutions of conjugates for (A) PEG-A and (B) PEG-B; C=1.0 wt%.

Conclusions

We report on the synthesis and solution properties of novel polymer conjugates. The conjugation of PEG with hydrophobic antioxidants gave rise to thermosensitive conjugates. The DLS and SAXS measurements show that by varying the PEG molecular weight the solution properties, including the LCST value, could be easily tuned across a broad temperature range (20-90 ºC), providing an ideal tool for the creation of thermosensitive polymers. Our results demonstrate that the conformation of the PEG conjugates is controlled by the balance of hydrophilic backbone and hydrophobic antioxidant substituent.

Acknowledgements

EMBL, Hamburg is acknowledged for beam time allocation. The authors acknowledge support from Grant Agency of the Czech Republic (Grant No. P208/10/1600). The authors also acknowledge financial support Nr. CZ09-DE06/2013-2014 from the ASCR - DAAD Programme PPP 2013-2014, and also support from the EU FP7 program, I3 access grant BioStruct-X, project Number 283570. We thank Nikolai Matushkin (Institute of Macromolecular Chemistry, Prague) for his help with preparation of picture of TOC file. The authors wish to express their sincere thanks Dr. Lenka Polakova (Institute of Macromolecular Chemistry, Prague) for providing chemical substances.

Notes and references

[a] Institute of Chemistry, Saint-Petersburg State University, Russia.

[b]Institute of Macromolecular Chemistry, AS CR, Heyrovsky Sq. 2, Prague, Prague 6, 162 06, Czech Republic.

[c]European Molecular Biology Laboratory, EMBL c/o DESY, Notkestrasse 85, Hamburg, D-22603, Germany.

Electronic Supplementary Information (ESI) available: Intensity weighted distribution function of nanoparticles obtained from DLS data for PEG-A (3K) at different temperatures; Scattered light intensity Is plotted as a function of solution temperature for PEG-A(3k) sample; Scattered light intensity I_s plotted as a function of solution temperature for PEG-A(6k) sample. See DOI: 10.1039/b000000x/

1 S. Zalipsky, *Bioconjugate Chem.,* 1995, **6**, 150-165.

2 O. Vittorio, G. Cirillo, F. Iemma, G. Di Turi, E. Jacchetti, M. Curcio, S. Barbuti, N. Funel, O. I. Parisi, F. Puoci and N. Picci, *Pharm. Res.*, 2012, **29**, 2601–2614.

3 R. Duncan and M. J. Vicent, *Advanced Drug Delivery Reviews*, 2013, **65**, 60–70.

4 M. Skodova, M. Hruby, S. K. Filippov, G. Karlsson, H. Mackova, M. Spirkova and K. Ulbrich, *Macromolecular Chemistry and Physics*, 2011, **212**, 2339–2348

5 C. Cummings, H. Murata, R. Koepsel and A. J. Russell *Biomacromolecules*, 2014, **15**, 763−771.

6 E. K. U. Larsen, M. B. L. Mikkelsen and N. B. Larse, *Biomacromolecules,* 2014, **15**, 894−899.

7 S. K. Filippov, Konak, C., Kopecková, P., Starovoytova, L., Spírková, M. and P. Stepanek, *Langmuir*, 2010, **26**, 4999–5006.

8 S. K. Filippov, J. M. Franklin, P. Konarev, P. Chytil, T. Etrych, A. Bogomolova, M. Dyakonova, C. Papadakis, A. Radulescu, K. Ulbrich, P. Stepanek and D. I. Svergun, *Biomacromolecules*, 2013, **14**, 4061-4070.

9 H. Sies, *Exp. Physiol.*, 1997, **82**, 291-295.

10 J. Prabhat, M. Flather, E. Lonn, M. Farkouh and S.Yusuf, *Ann. Intern. Med*., 1995, **123**, 860–872.

11 J. Tinkel, H. Hassanain and S. J.Khouri, *Cardiol Rev.*, 2012, **20**, 77-83.

12 *Antioxidant Polymers: Synthesis, Properties, and Applications*, Cirilo G., Iemma F.,Eds.; Wiley, **2012**.

13 O.Yu. Sergeeva, D. V. Aref'ev, N. S. Domnina and E. A. Komarova, *Russ. J. of Appl. Chem*+, 2005, **78**, 940-943.

14 S. K. Filippov, A. V. Lezov, O. Yu. Sergeeva, A. S. Olifirenko, S. B. Lesnichin, N. S. Domnina, E. A. Komarova, M. Almgren, G. Karlsson and P. Stepanek, *Eur. Polym. J.*, 2008, **44**, 3361–3369.

15 S. K. Filippov, A. S. Komolov, O. Yu. Sergeeva, A. S. Olifirenko, S. B. Lesnichin, E. A. Komarova, B. A. Loginov and A. V Lezov, *Polym. Sci. Ser. A*+, 2009, **51**, 161–167.

16 D.V. Aref'ev, N.S. Domnina, E.A. Komarova and A.Yu. Bilibin, *Eur. Polym. J.*, 1999, **35**, 279-284.

17 D.V. Aref'ev, N.S. Domnina, E.A. Komarova and A. Yu. Bilibin, *Eur. Polym. J.*, 2000, **36**, 857-860.

18 G. Cirillo, F. Puoci, F. Iemma, M. Curcio, O.I. Parisi, U.G. Spizzirri, , I. Altimari and N. Picci, *Pharmaceutical Development and Technology*, 2012, **17**, 466-476

19 J. Rena, Q. Li, F. Donga, Y. Fenga and Z. Guoa, *International Journal of Biological Macromolecules*, 2013, **53**, 77– 81

20 J. Tong, X. Yi, R. Luxenhofer, W. A. Banks, R. Jordan, M. C. Zimmerman and A. V. Kabanov, *Mol. Pharmaceutics*, 2013, **10**, 360−377.

21 D.V. Aref'ev, I. S. Belostotskaya, V. B. Vol'eva, N.S. Domnina, N. L. Komissarova, O. Yu. Sergeeva and R.S. Khrustaleva, *Russian Chemical Bulletin*, 2007, **56**, 781-790.

22 P. S. Vlasov, O. Yu. Sergeeva, N. S. Domnina, I. Yu. Chukicheva, E. V. Buravlev and A. V. Kuchin, *Chemistry of Natural Compounds*, 2012, **48**, 531-534

23 Ward, M. A.; Georgiou, T. K., Polymers, 2011, 3, 1215-1242.

24 V. O. Aseyev, H. Tenhu and F. M. Winnik, *Adv. Polym. Sci.*, 2006, **196**, 1–85.

25 D. Christova, R.Velichkova, W. Loos, E. J. Goethals and F. Du Prez, *Polymer*, 2003, **44**, 2255–2261.

26 Hinrichs, W. L. J.; Schuurmans-Nieuwenbroek, N. M. E.; Van De Wetering, P.; Hennink, W. E. J. Controlled Release 1999, 60 (2-3), 249-259.

27 Raduan, N. H.; Horozov, T. S.; Georgiou, T. K. Soft Matter 2010, 6 (10), 2321-2329.

28 Bütün, V.; Armes, S. P.; Billingham, N. C. Polymer 2001, 42 (14), 5993-6008.

29 Hoogenboom, R.; Thijs, H. M. L.; Jochems, M. J. H. C.; Van Lankvelt, B. M.; Fijten, M. W. M.; Schubert, U. S. Chem. Commun. 2008, (44), 5758-5760.

30 Furyk, S.; Zhang, Y.; Ortiz-Acosta, D.; Cremer, P. S.; Bergbreiter, D. E. J. Polym. Sci., Part A: Polym. Chem. 2006, 44 (4), 1492-1501.

31 Ward, M. A.; Georgiou, T. K., Soft Matter, 2012, 8, 2737-2745.

32 Ward, M. A.; Georgiou, T. K. J. Polym. Sci., Part A: Polym. Chem. 2013, 51(13), 2850–2859

33 M. Sedlak, P. Fallus, M. Steinhart, J. Gummel, P. Stepanek and S. K. Filippov, *Macromol. Chem. Physics*, 2013, **214**, 2841–2847.

34 O. V. Khutoryanskaya, Z. A. Mayeva, G. A. Mun and V. V. Khutoryanskiy, *Biomacromolecules*, 2008, **9**, 3353–3361.

35 M. T. Cook, G. Tzortzis, D. Charalampopoulos and V.V. Khutoryanskiy, *Int. J. Pharm.*, 2014, 466, 400-408.

36 D. E. Zhunuspayev, G. A. Mun, and V. V. Khutoryanskiy, *Langmuir*, 2010, **26**, 7590-7597.

37 O. Sedlacek, B. D. Monnery, S. K. Filippov, M. Hruby and R. Hoogenboom, *Macromol. Rapid Comm.*, 2012, **33**, 1648-1662.

38 A. H. Soeriyadi, G.-Z. Li, S. Slavin, M. W. Jones, C. M. Amos, C.R. Becer, M. R. Whittaker, D. M. Haddleton, C. Boyer and T. P. Davis, *Polymer Chemistry*, 2011, **2**, 815-822.

39 A. Bogomolova, M. Hruby, J. Panek, M. Rabyk, S. Turner, S. Bals, M. Steinhart, A. Zhigunov, P. Stepanek and S. K. Filippov, *J. Appl. Chrystallogr.*, 2013, **46**, 1690 –1698.

40 K. Bebis, M. W. Jones, D. M. Haddleton and M. I. Gibson, *Polymer Chemistry*, 2011, **2**, 975-982.

41 Salzinger, S., Huber, S., Jaksch, S., Busch, P., Jordan, R., & Papadakis, C. M. (). Colloid and Polymer Science, 2011, **290**, 385–400.

42 M. Hruby, S. K. Filippov, J. Panek, M. Novakova, H. Mackova, J. Kucka, D. Vetvicka and K. Ulbrich, *Macromol. Biosci.*, 2010, **10**, 916-924.

43 V. San Miguel, A. J. Limer, D. M. Haddleton, F. Catalina and C. Peinado, *European Polymer Journal,* 2008, **44**, 3853-3863

44 A. M. Bivigou-Koumba, E. Görnitz A. Laschewsky, P. Buschbaum, and C. M. Papadakis, *Colloid and Polymer Science*, 2010, **288**, 499–517.

45 M. Hruby, S. K. Filippov, J. Panek, M. Skodova, H. Mackova, J. Kucka and K. Ulbrich, *J. Control. Release*, 2010, **148**, 60-62.

46 S. K. Filippov, O. Sedlacek, A. Bogomolova, M. Vetrik, D. Jirak, J. Kovar, J. Kucka, S. Bals, S. Turner, P. Stepanek and M. Hruby, *Macromol. Biosci.*, 2012, **12**, 1731–1738.

47 S. K. Filippov, P. Chytil, P. Konarev, M. Dyakonova, C. M. Papadakis, A. Jigounov, J. Plestil, P. Stepanek, T. Etrych, K. Ulbrich and D. Svergun, *Biomacromolecules*, 2012, **13**, 2594–2604.

48 Ward, M. A.; Georgiou, T. K. J. Polym. Sci., Part A: Polym. Chem. 2010, 48 (4), 775-783.

49 Mun, G. A.; Nurkeeva, Z. S.; Beissegul, A. B.; Dubolazov, A. V.; Urkimbaeva, P. I.; Park, K.; Khutoryanskiy, V. V. Macromol. Chem. Phys. 2007, 208 (9), 979-987.

50 Mun, G. A.; Nurkeeva, Z. S.; Akhmetkalieva, G. T.; Shmakov, S. N.; Khutoryanskiy, V. V.; Lee, S. C.; Park, K. J. Polym. Sci., Part B: Polym. Phys. 2006, 44 (1), 195-205.

51 Zhao, X. L.; Liu, W. G.; Chen, D. Y.; Lin, X. Z.; Lu, W. W. Macromol. Chem. Phys. 2007, 208 (16), 1773-1781.

52 Ward, M. A.; Georgiou, T. K. Soft Matter 2012, 8 (9), 2737-2745.

53 Ward, M. A.; Georgiou, T. K. Polym. Chem. 2013, 4(6), 1893-1902.

Grafting density:

54 Chee, C. K.; Hunt, B. J.; Rimmer, S.; Rutkaite, R.; Soutar, I.; Swanson, L. Soft Matter 2009, 5 (19), 3701-3712.

55 Carter, S.; Hunt, B.; Rimmer, S. Macromolecules 2005, 38 (11), 4595-4603.

56 P. Stepanek and C. Konak, *Adv. Colloid Interfac*., 1984, **21**, 195-274.

57 B. Angelov, A. Angelova, S. K. Filippov, T. Narayanan, M. Drechsler, V. Nicolas, P. Stepanek, P. Couvreur and S. Lesieur, *J. Phys. Chem. Lett.*, 2013, **4**, 1959-1964.

58 D. Gromadzki, S. K. Filippov, M. Netopilik, R. Makuska, A. Jigounov, J. Plestil, J. Horsky, and P. Stepanek, *Eur. Polym. J.*, 2009, **45**, 1748-1758.

59 B. Angelov, A. Angelova, S. K. Filippov, G. Karlsson, N. Terrill, S. Lesieur and P.Stepanek, *Soft Matter*, 2011, **7**, 9714-9720.

60 J. B. Gilroy, P. A. Rupar, G. R. Whittell, L. Chabanne, N. J. Terrill, M. A. Winnik, I. Manners and R.M. Richardson, *Journal of the American Chemical Society*, 2011, **133**, 17056-17062.

61 L. A. Cohen and W. M. Jones, *JACS*, 1962, **84**, 1629.

62 J. Jakes, *J. Phys. (Paris)*, 1988, **38**, 1305-1316.

63 Stepanek, P. *In Dynamic Light Scattering: The Method and Some Applications*; Brown, W., Eds.; Clarendon Press: Oxford, U.K., **1993**; 175-241.

64 P. Konarev, V. Volkov, A. Sokolova, M. Koch and D. Svergun, *J. Appl. Crystallogr.*, 2003, **36**, 1277-1282.

65 C. E. Blanchet, A. V. Zozulya, A. G. Kikhney, D. Franke, P. V. Konarev, W. Shang, R. Klaering, B. Robrahn, C. Hermes, F. Cipriani, D. I. Svergun and M. Roessle, *Journal of Applied Crystallography*, 2012, **45**, 489–495.

66 H. Pasch and W. Schrepp, *MALDI-TOF Mass Spectrometry of Synthetic Polymers*, Springer-Verlag, Berlin Heidelberg New York, 2003.

67 H. Yamakawa, *Modern Theory of Polymer Solutions*, Harper and Row, New York, 1971, 262.

68 http://kur.web.psi.ch/sans1/SANSSoft/sasfit.html.

